Geochemistry of diogenites: Still more diversity in their parental melts

Jean-Alix J-A Barrat, A. Yamaguchi, R.C. Greenwood, M. Benoit, Joseph Cotten, Marcel Bohn, I.A. Franchi

▶ **To cite this version:**

Jean-Alix J-A Barrat, A. Yamaguchi, R.C. Greenwood, M. Benoit, Joseph Cotten, et al.. Geochemistry of diogenites: Still more diversity in their parental melts. Meteoritics and Planetary Science, 2008, 43 (11), pp.1759-1775. insu-00358210

HAL Id: insu-00358210

https://hal-insu.archives-ouvertes.fr/insu-00358210

Submitted on 26 Feb 2013

HAL is a multi-disciplinary open access archive for the deposit and dissemination of scientific research documents, whether they are published or not. The documents may come from teaching and research institutions in France or abroad, or from public or private research centers.

L'archive ouverte pluridisciplinaire **HAL**, est destinée au dépôt et à la diffusion de documents scientifiques de niveau recherche, publiés ou non, émanant des établissements d'enseignement et de recherche français ou étrangers, des laboratoires publics ou privés.

The Meteoritical Society

Meteoritics & Planetary Science 43, Nr 11, 1759–1775 (2008)
Abstract available online at http://meteoritics.org

Geochemistry of diogenites: Still more diversity in their parental melts

J. A. BARRAT[1, 2*], A. YAMAGUCHI[3], R. C. GREENWOOD[4], M. BENOIT[2, 5], J. COTTEN[1, 2], M. BOHN[1, 2], and I. A. FRANCHI[4]

[1]Université Européenne de Bretagne, France
[2]Université de Brest, CNRS UMR 6538 (Domaines Océaniques), I.U.E.M., Place Nicolas Copernic, 29280 Plouzané Cedex, France
[3]Antarctic Meteorite Research Center, National Institute of Polar Research, 1-9-10 Kaga, Itabashi, Tokyo 173-8515, Japan
[4]PSSRI, The Open University, Walton Hall, Milton Keynes MK7 6AA, UK
[5]Université Paul Sabatier, CNRS-UMR 5562, Observatoire Midi-Pyrénées, 14 avenue Edouard Belin, 31400 Toulouse, France
[*]Corresponding author. E-mail: barrat@univ-brest.fr

(Received 27 March 2008; revision accepted 30 June 2008)

Abstract–We report on the major and trace element abundances of 18 diogenites, and O-isotopes for 3 of them. Our analyses extend significantly the diogenite compositional range, both in respect of Mg-rich (e.g., Meteorite Hills [MET] 00425, MgO = 31.5 wt%) and Mg-poor varieties (e.g., Dhofar 700, MgO = 23 wt%). The wide ranges of siderophile and chalcophile element abundances are well explained by the presence of inhomogeneously distributed sulfide or metal grains within the analyzed chips. The behavior of incompatible elements in diogenites is more complex, as exemplified by the diversity of their REE patterns. Apart from a few diogenite samples that contain minute amounts of phosphate, and whose incompatible element abundances are unlike the orthopyroxene ones, the range of incompatible element abundances, and particularly the range of Dy/Yb ratios in diogenites is best explained by the diversity of their parental melts. We estimate that the FeO/MgO ratios of the diogenite parental melts range from about 1.4 to 3.5 and therefore largely overlap the values obtained for non-cumulate eucrites. Our results rule out the often accepted view that all the diogenites formed from parental melts more primitive than eucrites during the crystallization of a magma ocean. Instead, they point to a more complex history, and suggest that diogenites were derived from liquids produced by the remelting of cumulates formed from the magma ocean.

INTRODUCTION

In 2011 the Dawn spacecraft will begin to map its first target in the asteroid belt: the asteroid 4 Vesta. Vesta is the second largest object by mass in the asteroid belt and astronomical observations suggest that it is covered by magmatic rocks, such as basalts and pyroxenites. Since the seventies (McCord et al. 1970), it has been proposed that Vesta is the source of the most abundant group of achondrites, namely the howardite, eucrite, and diogenite (HED) suite. Eucrites are basic rocks that display magmatic textures and chemical compositions indicating formation as lava flows or intrusions. They are generally regarded as being samples of the upper crustal lithologies from 4 Vesta. Diogenites are orthopyroxene-rich cumulates, while howardites are polymict breccias containing both eucritic and diogenitic lithologies.

HEDs offer a unique opportunity to understand the processes that generated igneous activity during the early history of a small body. It has been proposed that the diversity of eucritic melts is the result of the combined effects of various degrees of partial melting and fractional crystallization within Vesta's mantle (e.g., Stolper 1977; Consolmagno and Drake 1977; Mittlefehldt 1979; Mittlefehldt and Lindstrom 2003). In contrast, others have suggested that magmatic activity on the HED parent body was dominated by a large-scale melting event, which generated a global magma ocean (e.g., Ikeda and Takeda 1985; Righter and Drake 1997; Ruzicka et al. 1997; Takeda 1997; Warren 1997; Greenwood et al. 2005). According to this view, the chemistry of eucritic melts can be explained in terms of fractional crystallization processes (e.g., Stolper 1977; Warren and Jerde 1987). Contamination of the eucritic magmas by liquids derived by partial melting of the asteroid's crust has also been proposed (Barrat et al. 2007). The study of HED cumulate lithologies provides a complementary view of early magmatic processes on Vesta. Although it is generally accepted that a few gabbros, the cumulate eucrites, formed from "ordinary" eucritic melts (Treiman 1997; Barrat et al.

© The Meteoritical Society, 2008. Printed in USA.

2000a; Saiki et al. 2001; Barrat 2004), the origin of the diogenites and the composition of their parental melts remain unresolved (e.g., Mittlefehldt 1994; Fowler et al. 1994, 1995; Shearer et al. 1997; Barrat 2004). Diogenites are believed to be a major lithological component of Vesta. Their relative abundance among the HED group, and astronomical observations of the Vesta's surface, imply that they comprise a significant part of the crust which has been excavated and exposed by large impacts (Gaffey 1997; Binzel et al. 1997). Improving our understanding of diogenite genesis is now a critical task if we are to gain a better overall picture of the magmatic processes that operated on Vesta. In this paper, we report on the geochemistry of 18 diogenites, and discuss the diversity of their parent melts.

ANALYTICAL METHODS

Powders were prepared using a boron-carbide mortar and pestle. They were dissolved in screw-top teflon vessels (Savillex) at about 130 °C for five days using 5 ml of concentrated HF, and 2 ml of concentrated HNO_3. After evaporation to dryness of the acid mixture, approximately 2 ml of HNO_3 was added, and the vessels were capped and placed back on the hot plate and left overnight. The samples were then dried again, and taken up in ~20 g of 6 M HCl ("mother solutions"). Only reagents double-distilled in quartz or teflon sub-boilers were used. Abundances of both major and trace elements were analyzed using aliquots of the same mother solutions for all samples.

The concentrations of TiO_2, Al_2O_3, Cr_2O_3, FeO, MnO, MgO, and CaO were determined by ICP-AES using a modified Jobin Yvon spectrometer, following the procedures of Cotten et al. (1995). For major element concentrations the accuracy is better than 3%. Na_2O, K_2O, and P_2O_5 were determined but their concentrations were insignificant for all the samples (<0.02 wt%) and are not given here.

Whole rock trace element abundances were determined using an inductively coupled plasma-mass spectrometer (ICP-MS) (Thermo Element 2) at Institut Universitaire Européen de la Mer (IUEM), Plouzané (Barrat et al. 2007). The results for the international ultramafic standards PCC1 and JP1 are given in Table 1 relative to our best estimate of the USGS basalt BHVO2, which is based on our own measurements and values from the literature. (In the event of future change to these BHVO2 values, the data need only to be corrected by the ratio of the new and old values). The standard data are in excellent agreement with previously published data sets (e.g., Makishima and Nakamura 1997; Ionov et al. 2005), confirming the very good quality of our calibration procedures. Based on standard measurements (see Table 1) and many sample duplicates, trace element concentration reproducibility is generally better than 5%. The reproducibility for low Nb and Eu concentrations is sometimes not so good. In the case of Eu in JP1, the dispersion is explained by the high Ba/Eu ratio (about 2500) of this peridotite (i.e., the contribution of the $^{135}Ba^{16}O$ interference on the ^{151}Eu peak was important and difficult to correct [e.g., Barrat et al. 2000b]).

Three diogenite samples, Northwest Africa (NWA) 4272, Dhofar 700, and Asuka- (A) 881548, were analyzed for oxygen isotopes as part of this study by infrared laser-assisted fluorination (Miller et al. 1999). O_2 was liberated by heating the samples using an infrared CO_2 laser (10.6 μm) in the presence of 210 torr of BrF_5. After fluorination, the O_2 released was purified by passing it through two cryogenic nitrogen traps and over a bed of heated KBr. O_2 was analyzed using a Micromass Prism III dual inlet mass spectrometer. System precision (2σ), based on replicate analyses of the international standard UWG-2 garnet is: ±0.06‰ for $\delta^{17}O$; ±0.13‰ for $\delta^{18}O$; ±0.02‰ for $\delta^{17}O$. Oxygen isotope analyses are reported in standard δ notation where $\delta^{18}O$ has been calculated as: $\delta^{18}O = \{[(^{18}O_{sample}/^{16}O_{sample})/(^{18}O_{ref}/^{16}O_{ref})]-1\} \times 1000$, and similarly for $\delta^{17}O$ using $^{17}O/^{16}O$ ratio. $\Delta^{17}O$ is calculated using a linearized format, where $\Delta^{17}O = 1000 \ln [1 + (\delta^{17}O/1000)] - \lambda 1000 \ln [1 + (\delta^{18}O/1000)]$ where $\lambda = 0.5247$ (Miller 2002). To assess the influence of weathering, Dhofar 700 and A-881548 were leached using a solution of ethanolamine thioglycollate (Cornish and Doyle 1984) and then washed and dried prior to fluorination. This treatment removes iron oxides, hydroxides and metallic iron, but not silicate-bound iron. An aliquot of Dhofar 700 was also washed in dilute HCl.

RESULTS AND DISCUSSION

The major and trace element characteristics of diogenites and their orthopyroxenes have been extensively described elsewhere (e.g., Fredriksson et al. 1976; Fukuoka et al. 1977; Mittlefehldt 1994) and will not be repeated here except for a brief overview of the factors controlling their composition. Eighteen diogenites, mainly collected in Antarctica, have been analyzed for major and trace elements during the course of this study. Details of the samples studied, including the composition of major mineral phases, are given in Table 2. The results of major and trace element analyses are given in Tables 3 and 4, and of oxygen isotope analysis in Table 5.

Factors Controlling the Composition of Diogenites

Previous geochemical studies of diogenites have shown that their major element concentrations are strongly controlled by the composition of their orthopyroxenes, in agreement with their nearly monomineralic nature (e.g., Fredriksson et al. 1976; Fukuoka et al. 1977; Mittlefehldt 1994, 2002). Limited deviations from the orthopyroxene compositions are generally well explained by the involvement of small amounts of chromite, olivine or plagioclase. While the results of our study lend additional

Table 1. Isotopes selected for analysis, resolution modes, trace element abundances for USGS BHVO2 basalt (best estimate), for PCC1, JP1 peridotites obtained during the course of this study (three different dissolutions for each standards), and estimate of 1σ analytical uncertainty for a typical diogenite sample (e.g., Johnstown or Dhofar 700) based on replicate analyses of the same mother solution and of homogeneous geochemical reference standards.

	Isotopes	Resolution	BHVO2 (µg/g)	PCC1 (µg/g)	RSD% n = 3	JP1 (µg/g)	RSD% n = 3	Uncert.
Sc	45	MR	32.3	8.37	0.8	7.25	3.3	<4%
Ti	47	MR	16364	26	3.4	19.9	8	<4%
V	51	MR	317	25.7	1.1	21.65	2.8	<2%
Mn	55	MR	1290	849	1.2	860	2.3	<3%
Co	59	MR	45	103	1.1	104	6.1	<2%
Ni	60, 61, 62	MR	121	2171	1.1	2211	4.8	<3%
Cu	63, 65	MR	123	6.71	0.6	3.63	17.6	<5%
Zn	66, 68	MR	101	34.8	1.9	37.66	5.5	<10%
Ga	89	MR	20.6	0.51	1.1	0.47	1.8	<3%
Sr	88	MR	396	0.344	2.3	0.527	4.7	<3%
Y	89	LR	28	0.082	0.8	0.1	3.7	<1%
Zr	90, 91	LR	178	0.14	5.6	5.39	1.9	<7%
Nb	93	LR/MR	19.3	0.02	14.1	0.04	35.2	<15%
Ba	135	LR	131	0.79	1.9	10.04	1.1	<2%
La	139	LR	15.2	0.0293	2.4	0.0271	1.7	<3%
Ce	140	LR	37.5	0.0547	2	0.0597	2.4	<3%
Pr	141	LR	5.31	0.00662	3.3	0.00716	4.5	<3%
Nd	143, 146	LR	24.5	0.0255	2.6	0.0298	2.4	<3%
Sm	147, 149	LR	6.07	0.00458	2.5	0.00726	5.1	<3%
Eu	151	LR	2.07	0.00079	2	0.00385	9	<3%
Gd	157	LR	6.24	0.00513	3.2	0.0085	15.1	<3%
Tb	159	LR	0.94	0.00101	5.1	0.00166	8.4	<3%
Dy	163	LR	5.31	0.00921	1.6	0.0135	3.2	<3%
Ho	165	LR	0.97	0.00256	1.3	0.00316	5.9	<2%
Er	167	LR	2.54	0.011	2.3	0.0116	2.9	<3%
Yb	174	LR	2	0.0214	1.6	0.0194	0.9	<2%
Lu	175	LR	0.27	0.00421	1.3	0.00352	1.9	<2%
Hf	177, 178	LR	4.28	0.00379	6.4	0.113	0.6	<5%
Th	232	LR	1.21	0.011	2.3	0.0122	1	<3%
U	238	LR	0.41	0.0042	4.4	0.0122	1.2	<3%

support for this correlation, our new analyses also significantly extend the compositional range of diogenite compositions to both Mg-rich (e.g., MET 00425, MgO = 31.5 wt%) and Mg-poor examples (e.g., Dhofar 700, MgO = 23 wt%). The behavior of trace elements in diogenites is much more complex, as exemplified by siderophile and highly incompatible elements. Johnstown, which has been repeatedly analyzed in the past (e.g., Floran et al. 1981; Mittlefehldt 1994; Fowler et al. 1995, and this study), illustrates this behavior:

1. Johnstown displays a wide range of Ni and Co abundances (Ni = 37–460 µg/g, Co = 12–85 µg/g, Fig. 1). Floran et al. (1981) have proposed that this range could be explained by the involvement of a foreign meteoritic component in this breccia. On the other hand, high siderophile abundances are not just restricted to matrix-rich material, so that some orthopyroxene clasts can also exhibit high Ni and Co abundances. Therefore, the behavior of these elements are more likely explained by traces of metal contained within orthopyroxene crystals. A similar explanation has been proposed by Mittlefehldt (2000) for Elephant Moraine (EET) A79002. Clearly, if this nugget effect is correct, it will need to be taken into account, not only for the interpretation of highly siderophile element abundances in bulk rocks, but also in dating studies using Hf-W or Re-Os systematics. Similarly, sulfide grains can be inhomogeneously distributed within orthopyroxene crystals and this might explain the variation in chalcophile elements seen in diogenites (e.g., Cu = 0.1 to 8.8 µg/g in the samples we have analyzed [Tables 3 and 4]).
2. Orthopyroxene displays very low partition coefficients for incompatible elements (Schwandt and McKay 1998), consequently orthopyroxenites are extremely poor in light REEs or Th. Diogenites also show this behavior such that most of them display REE patterns with light REE abundances largely below the chondritic level. Unfortunately, such low concentrations are extremely sensitive to contributions from enriched phases, such as

Table 2. Details of meteorite samples studied.

	Opx	Ol	Pl	Source	# or split	Comments
Falls						
Bilanga	Fs_{21}		$An_{46–92}$	A. Carion		
Johnstown	Fs_{24}	Fa_{29}	An_{87}	AMNH	#2497	Large clast
Hot desert finds						
Tatahouine	Fs_{23}			J. A. Barrat		Unbrecciated
Dho 700	Fs_{31}	$Fa_{32–37}$	$An_{89–95}$	M. Farmer		Unbrecciated
NWA 4272	Fs_{22}		$An_{81–86}$	M. Franco		
Antarctic finds						
A-881526	Fs_{25}			NIPR	,56	
A-881548	Fs_{22}	Fa_{24}		NIPR	,23	
A-881839	Fs_{27}		$An_{88–92}$	NIPR	,22	
EETA79002	$Fs_{19–28}$	Fa_{24}		MWG	,174	Dark chip
GRO 95555	Fs_{23}			MWG	,30 ,36	Unbrecciated
LAP 02216	Fs_{23}			MWG	,16 ,17	
LAP 03569	Fs_{22}	Fa_{27}		MWG	,11	
LAP 03630	Fs_{24}			MWG	,11	
MET 00422	Fs_{22}			MWG	,10	
MET 00424	Fs_{27}	Fa_{29}		MWG	,16	
MET 00425	Fs_{15}			MWG	,11	
MET 00436	Fs_{26}			MWG	,17	
MIL 03368	Fs_{27}			MWG	,8	

Source abbreviations are: AMNH = American Museum of Natural History, New York; MWG = NASA Meteorite Working Group; NIPR = National Institute of Polar Research, Tokyo.

those produced during hot desert weathering (e.g., Barrat et al. 1999, 2006), accessory phases (e.g., phosphates, plagioclase), a trapped melt fraction, or any foreign fragments (e.g., chondritic meteorites, plagioclase or small eucritic clasts in diogenitic breccias, see Lomena et al. [1976], Hewins [1988] and Mittlefehldt [1994]). Therefore, the abundances of light REEs in orthopyroxene compared to bulk rocks can differ significantly. Johnstown is again a perfect illustration of this effect (Fig. 2). The La concentrations displayed by the orthopyroxenes and the chips of this meteorite vary by more than two orders of magnitude, and a trapped melt contribution was proposed by Floran et al. (1981). We have analyzed a large orthopyroxene clast extracted from Johnstown, our results for this material falling within the range of literature values (e.g., Floran et al. 1981; Mittlefehldt 1994). The REE abundances we have obtained, are significantly higher than the orthopyroxene concentrations (Fowler et al. 1995), and confirm the involvement of a light REE-enriched component. The involvement of such a light REE-enriched component is also seen in Aïoun el Atrouss, Roda, Allan Hills (ALH) A77256 when bulk rock and orthopyroxene analyses are compared (Mittlefehldt 1994; Fowler et al. 1995).

3. The contribution of enriched components is not the only parameter that can explain the variation displayed by incompatible element variation in bulk diogenites. REE element distributions indicate that diogenites formed from a variety of parental melts (Mittlefehldt 1994; Fowler et al. 1995; Shearer et al. 1997), some of which were significantly enriched in heavy REEs (Barrat 2004). This point is discussed below.

Non-Antarctic Diogenites

Bilanga

The mineralogy of this recent fall has been described by Domanik et al. (2004). A large fragment (3.4 g) had previously been powdered and analyzed for REE elements (Barrat 2004). We reanalyzed a split of this powder, and present here the first complete analysis (major and trace elements) of this meteorite. The major element abundances are very similar to the average orthopyroxene composition ($En_{78.3}$, Domanik et al. 2004), suggesting that other known phases in Bilanga (chromite, diopside, plagioclase) were present in only very minor amounts in our fragment. Trace element abundances are in the range of other diogenites (Fig. 3), although as pointed out by Mittlefehldt (2002) this meteorite is poor in Sc (7.3 μg/g).

Tatahouine

The fall of the Tatahouine diogenite took place in 1931, with ten or so kilograms of material being recovered soon afterwards (Lacroix 1932). The strewn field was rediscovered by Alain Carion in 1994, and many other fragments have since been collected. The sample analyzed here was collected by one of us (JAB) in 2000, and is slightly weathered, as shown by its high Ba and Sr concentrations. Despite these

Table 3. Major and trace element abundances of non-Antarctic diogenites (oxides in wt%, traces elements in μg/g).

			Dhofar 700			NWA	
	Bilanga	Johnstown	W.R.	Residue	Residue	4272	Tatahouine
Mass (g)	0.2306	0.2357	0.1295	0.2341	0.2341	0.2038	0.2034
TiO_2	0.09	0.14	0.07	0.07		0.19	0.08
Al_2O_3	0.87	1.1	1.17	0.83		1.13	0.59
Cr_2O_3	0.86	0.89	0.8	0.8		0.59	0.93
FeO	13.5	15.93	19.98	20.05		14.94	15.48
MnO	0.43	0.5	0.74	0.75		0.47	0.5
MgO	29.7	26.2	23	23.1		27.9	28.2
CaO	0.97	1.45	2.66	2.27		1.47	0.78
Sc	7.25	15.63	29.14	29.64		14.34	13.33
Ti	461	756	374	373		968	416
V	88	99	152	144		75	104
Mn	2879	3400	4923	4948		3118	3289
Co	20	14.9	13.3	10.1		7.7	11.9
Ni	8.5	30	24.8	8.7		6.6	8.5
Cu	0.14	1.55	2.28	0.07		0.33	0.34
Zn	0.5	1.5	1.77	0.72		0.7	0.1
Ga	0.17	0.2	0.18	0.12		0.18	0.15
Sr	0.95	1.54	9.95	0.17		2.36	0.8
Y	0.99	1.69	0.88	0.91	0.91	2.73	0.25
Zr	0.72	2.42	0.52	0.28		3.55	0.15
Nb	0.14	0.36	0.021	0.011		0.39	0.044
Ba	0.21	3.03	1.49	0.08		1.75	0.43
La	0.0113	0.126	0.057	0.0028	0.0025	0.131	0.0067
Ce	0.0487	0.345	0.133	0.0127	0.0119	0.423	0.0144
Pr	0.0101	0.0538	0.0119	0.0023	0.0022	0.071	0.002
Nd	0.0693	0.288	0.0444	0.0189	0.0183	0.395	0.0096
Sm	0.0426	0.105	0.0191	0.0171	0.0170	0.158	0.0034
Eu	0.0041	0.0107	0.0035	0.0008	0.0007	0.0178	0.0006
Gd	0.0746	0.147	0.0482	0.0471	0.0503	0.245	0.0069
Tb	0.0178	0.0311	0.0126	0.0129	0.0138	0.053	0.0021
Dy	0.145	0.25	0.113	0.116	0.122	0.403	0.0247
Ho	0.0371	0.0618	0.0313	0.0321	0.0326	0.099	0.0081
Er	0.119	0.201	0.106	0.108	0.111	0.307	0.0341
Yb	0.129	0.223	0.126	0.126	0.129	0.326	0.0604
Lu	0.0211	0.0369	0.0198	0.0198	0.0202	0.053	0.0117
Hf	0.025	0.068	0.019	0.014		0.108	0.003
Th	0.0013	0.0205	0.0016	0.0003		0.0258	0.001
U	0.0022	0.0136	0.018	0.0001		0.0052	0.0007
(La/Sm)n	0.14	0.65	1.62	0.09	0.09	0.45	1.06
(Gd/Lu)n	0.43	0.48	0.29	0.29	0.31	0.56	0.07
Eu/Eu^*	0.22	0.26	0.35	0.09	0.07	0.27	0.37

differences, the results are very similar to those obtained on samples collected in 1931 (Mittlefehldt 1994; Barrat et al. 1999), as exemplified by its REE pattern that shows a strong heavy REE enrichment (Fig. 4a).

Dhofar 700

This unbrecciated diogenite is slightly weathered and displays some fractures filled with secondary carbonates and Fe-hydroxides. We powdered about half a gram of Dhofar 700, and analyzed two different splits. We directly dissolved the first one, and the other was leached for one hour in hot (100 °C) sub-boiled 6 N HCl in order to remove the terrestrial secondary phases. The residue was rinsed five times in ultrapure water prior to analysis. Very similar results were obtained for major elements for both splits (Table 3). However, the residue displays slightly lower Al_2O_3, CaO, Ni, Cu, and Zn suggesting that small amounts of plagioclase, sulfide and metal were removed during the leaching procedure. Furthermore, Sr, Ba, Zr, and the light REE abundances have been significantly reduced, thus indicating that our leaching procedure has efficiently removed *most* of the products of terrestrial weathering. The major and minor element abundances are similar to the average orthopyroxene composition, and it can therefore be inferred that the trace

Table 4. Major and trace element abundances of Antarctic diogenites (oxides in wt%, traces elements in μg/g).

	EETA 79002,174	LAP 02216,17	LAP 02216,16	LAP 03630,11	MIL 03368,8	Asuka 881526,56	LAP 03569,11	MET 00422,10
Mass (g)	0.1802	0.1638	0.1487	0.1612	0.1666	0.1306	0.1896	0.1788
TiO_2	0.10	0.10	0.09	0.07	0.12	0.13	0.11	0.05
Al_2O_3	0.79	0.76	0.65	0.67	1.00	1.04	0.92	0.56
Cr_2O_3	0.77	0.86	0.75	0.74	1.12	0.81	1.03	0.99
FeO	17.60	17.06	17.07	16.21	17.08	16.20	17.06	18.00
MnO	0.51	0.52	0.53	0.57	0.55	0.52	0.51	0.60
MgO	27.44	27.23	27.41	27.26	26.10	27.30	28.85	26.20
CaO	1.17	1.16	1.19	1.19	1.62	1.34	1.44	0.92
Sc	13.26	13.21	12.73	13.33	13.68	14.20	12.95	15.47
Ti	539	519	470	375	605	629	551	256
V	96	100	92	97	156	92	99	120
Mn	3461	3376	3496	3666	3637	3122	3258	3973
Co	23.1	19.5	29.8	6.8	19.8	10.3	28.8	25.0
Ni	78.9	48.3	88.0	6.9	11.4	21.0	45.0	19.9
Cu	7.45	4.00	4.70	0.49	2.55	0.63	2.49	1.74
Zn	0.6	0.1	–	0.8	0.3	0.23	0.2	0.8
Ga	0.11	0.10	0.093	0.077	0.19	0.14	0.12	0.20
Sr	0.41	0.27	0.27	0.23	0.24	0.51	0.59	0.14
Y	0.78	0.78	0.66	0.58	1.00	1.33	0.96	0.23
Zr	0.62	0.68	0.44	0.47	0.55	1.07	0.90	0.16
Nb	0.037	0.048	0.039	0.019	0.030	0.041	0.079	0.024
Ba	0.16	0.13	0.09	0.06	0.10	0.02	0.33	0.08
La	0.0156	0.0160	0.0107	0.0070	0.0139	0.0279	0.0321	0.0074
Ce	0.0468	0.0516	0.0326	0.0244	0.0403	0.082	0.0879	0.0193
Pr	0.0078	0.0090	0.0054	0.0045	0.0068	0.014	0.0127	0.0027
Nd	0.0483	0.0566	0.0379	0.0348	0.0454	0.088	0.0734	0.0153
Sm	0.0250	0.0258	0.0187	0.0203	0.0262	0.0500	0.0327	0.0063
Eu	0.0042	0.0039	0.0030	0.0023	0.0031	0.0084	0.0064	0.0014
Gd	0.0481	0.0515	0.0391	0.0366	0.0550	0.0932	0.0643	0.0120
Tb	0.0118	0.0118	0.0096	0.0089	0.0143	0.0224	0.0150	0.0030
Dy	0.104	0.101	0.0851	0.0770	0.128	0.184	0.125	0.0287
Ho	0.0286	0.0280	0.0237	0.0204	0.0355	0.0485	0.0337	0.0081
Er	0.0996	0.0945	0.0832	0.0707	0.1234	0.162	0.1159	0.0294
Yb	0.135	0.133	0.115	0.0956	0.163	0.212	0.152	0.0443
Lu	0.0232	0.0222	0.0201	0.0162	0.0270	0.0356	0.0261	0.0081
Hf	0.023	0.025	0.017	0.017	0.022	0.040	0.032	0.005
Th	0.0017	0.0022	0.0013	0.0012	0.0016	0.0041	0.0041	0.0011
U	0.0006	0.0010	0.0005	0.0003	0.0010	0.0009	0.0012	0.0002
(La/Sm)n	0.34	0.34	0.31	0.19	0.29	0.30	0.53	0.63
(Gd/Lu)n	0.25	0.28	0.23	0.27	0.25	0.32	0.30	0.18
Eu/Eu^*	0.36	0.33	0.33	0.26	0.25	0.37	0.42	0.47

element abundances of the residue are also very close to those of the orthopyroxene fraction. The REE pattern of Dhofar 700 (Fig. 3) displays a strong depletion from Lu to La with a deep negative Eu anomaly ($Eu/Eu^* = 0.09$). The positive Ce anomaly ($Ce/Ce^* = 1.20$) is not an analytical artifact and suggests that minute amounts of secondary phases have survived the leaching procedure. Dhofar 700 is one of the most ferroan diogenites analyzed during the course of this study. In addition, its Sc abundance is very high (Sc = 29 μg/g), and is similar to concentrations measured in main group eucrites.

The bulk oxygen isotopic composition of Dhofar 700 has been determined on both untreated and acid washed samples (Table 5). The aliquots leached in dilute HCl and ethanolamine thioglycollate both display a consistent shift to lower $\delta^{18}O$ and $\delta^{17}O$ values when compared to the untreated sample (Table 5, Fig. 5). The heavy $\delta^{18}O$ and $\delta^{17}O$ composition of the untreated Dhofar 700 sample undoubtedly reflects the influence of hot desert weathering processes. The fact that both the HCl and ethanolamine thioglycollate leached aliquots are in reasonable agreement suggests that in both cases the weathered products have largely been removed

Table 4. *Continued.* Major and trace element abundances of Antarctic diogenites (oxides in wt%, traces elements in µg/g).

	MET	MET	Asuka-881839, 22			GRO	GRO	MET	Asuka
	00425,11	00436,17	W.R.	Residue	"Phosphate"	95555,30	95555,36	00424,16	881548,23
Mass (g)	0.1454	0.1208	0.1304	0.083		0.1475	0.1994	0.1414	0.1312
TiO_2	0.04	0.05	0.16			0.08		0.03	0.11
Al_2O_3	0.52	0.69	1.15			0.68		0.30	0.94
Cr_2O_3	0.74	4.05	0.82			0.94		0.55	0.59
FeO	11.6	21.27	18.72			16.31		20.39	16.96
MnO	0.38	0.69	0.65			0.55		0.71	0.49
MgO	31.45	23.62	23.8			27.38		25.36	28.3
CaO	0.54	0.76	2.56			1.15		0.76	1.17
Sc	6.39	15.62	21.57	19.95		11.54	11.50	16.63	12.72
Ti	197	256	886	910		411	458	113	557
V	77	348	125	135		120	125	94	99
Mn	2496	4540	4274	4472		3580	3609	4618	3208
Co	13.6	6.2	15.8	6.46		13.8	14.8	35.4	4.2
Ni	19.1	1.2	28	2.67		6.2	7.3	1.3	26.5
Cu	1.75	8.78	0.86	0.14		1.14	2.32	4.9	5.69
Zn	0.5	0.2	0.72	–		0.6	0.25	0.3	0.34
Ga	0.069	0.22	0.18	0.15		0.10	0.11	0.043	0.16
Sr	1.14	0.3	4.68	0.65	53496	0.63	0.67	<0,015	0.44
Y	0.37	0.15	2.98	2.56	5666	0.51	0.68	0.006	1.68
Zr	1.12	0.53	6.96	6.90		0.50	0.71	<0.1	1.79
Nb	0.100	0.072	0.47	0.38		0.049	0.058	<0.15	0.76
Ba	0.60	0.20	2.26	0.65	23130	0.12	0.41	<0.015	0.37
La	0.0563	0.0173	0.368	0.0861	3950	0.0267	0.0437	<0.001	0.061
Ce	0.164	0.0484	0.977	0.303	8942	0.0804	0.108	<0.002	0.277
Pr	0.0203	0.0068	0.151	0.0606	1176	0.0119	0.0143	<0.0005	0.057
Nd	0.107	0.0359	0.793	0.405	5322	0.0629	0.0732	<0,001	0.347
Sm	0.0364	0.0124	0.265	0.179	1161	0.0223	0.0296	<0,0005	0.131
Eu	0.0068	0.0022	0.043	0.0088	466	0.0059	0.0057	<0,0002	0.0078
Gd	0.0475	0.0169	0.348	0.269	1217	0.0346	0.0521	<0,0005	0.171
Tb	0.0087	0.0031	0.0655	0.0553	180	0.0078	0.0116	<0,0002	0.035
Dy	0.0599	0.0222	0.459	0.404	982	0.0668	0.0917	0.00036	0.253
Ho	0.0135	0.0052	0.108	0.0979	197	0.018	0.0234	0.00014	0.0612
Er	0.0404	0.0162	0.330	0.313	509	0.063	0.0803	0.00093	0.191
Yb	0.0442	0.0186	0.347	0.337	378	0.0882	0.105	0.00508	0.217
Lu	0.0071	0.00315	0.0551	0.0546	54.8	0.0152	0.0181	0.00145	0.0353
Hf	0.028	0.011	0.192	0.198		0.015	0.025	<0,005	0.044
Th	0.0141	0.0026	0.0496	0.0104	482	0.0033	0.0104	<0,001	0.009
U	0.002	0.0005	0.016	0.0105	85.5	0.0009	0.0019	<0,0004	0.021
$(La/Sm)_n$	0.84	0.76	0.75	0.26	1.84	0.65	0.93		0.25
$(Gd/Lu)_n$	0.81	0.65	0.76	0.6	2.69	0.28	0.36	<0,04	0.59
Eu/Eu^*	0.5	0.47	0.43	0.12	1.19	0.64	0.44		0.16

Table 5. Oxygen isotopes data for diogenites Dho 700, NWA 4272, and A-881548 (n = number of replicates).

Sample	Comments	n	$\delta^{17}O‰$	1σ	$\delta^{18}O‰$	1σ	$\Delta^{17}O‰$	1σ
Dhofar 700	Unwashed	2	1.86	0.03	3.97	0.1	–0.23	0.02
Dhofar 700	Washed thioglycolate	2	1.52	0.01	3.38	0.01	–0.25	0.01
Dhofar 700	Washed dilute HCl	1	1.57		3.45		–0.24	
A-881548	Unwashed	4	1.64	0.12	3.56	0.21	–0.23	0.02
A-881548	Washed thioglycolate	2	1.62	0.01	3.56	0.01	–0.24	0.01
NWA 4272	Unwashed	2	1.63	0.03	3.56	0.01	–0.23	0.02

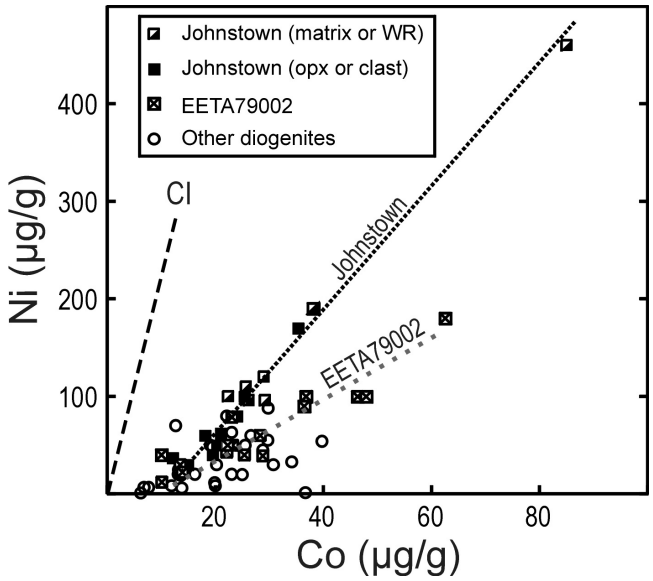

Fig. 1. Ni versus Co diagram for diogenites. The data are from Floran et al. (1981), Mittlefehldt (1994, 2000), Barrat et al. (2006), and this study.

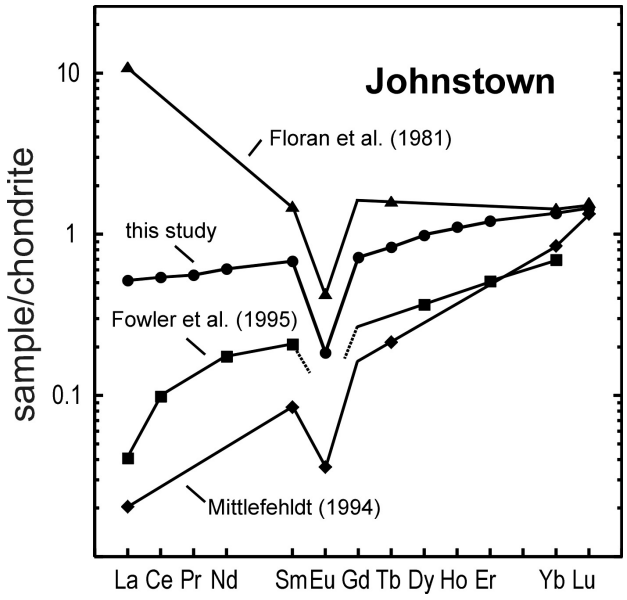

Fig. 2. REE concentrations for different samples of Johnstown vary greatly. The reference chondrite is from Evensen et al. (1978). The 2σ errors for the new analysis are equivalent to the size of the data points.

by these treatments. Only the result for ethanolamine thioglycollate treatment is plotted on Fig. 5. This shows that the oxygen isotope composition of Dhofar 700 is well within the range of previous measurements from diogenites (Clayton and Mayeda 1996; Wiechert et al. 2004; Greenwood et al. 2005).

Northwest Africa 4272

This diogenite is a relatively fresh hot desert find, and the fraction we have analyzed was apparently devoid of

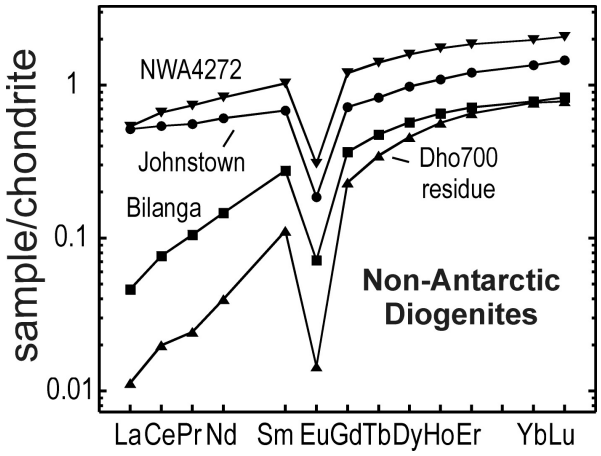

Fig. 3. REE patterns of selected non-Antarctic diogenites analyzed during the course of this study. The reference chondrite is from Evensen et al. (1978). The 2σ errors are equivalent to the size of the data points.

secondary phases. Its major and trace element abundances are very similar to our Johnstown clast (Table 3). We believe that an enriched component explains the shape of its REE pattern (Fig. 3) and the rather high light REE abundances. This interpretation is in agreement with petrographic observations. NWA 4272 exhibits an unusual texture with veins of calcic plagioclase (or interstitial plagioclase?) and minor diopside (Connolly et al. 2007) that are possible remnants of an interstitial melt. The O isotopic composition of this meteorite (Table 5) is well within the range of previous measurements from diogenites (Clayton and Mayeda 1996; Wiechert et al. 2004; Greenwood et al. 2005).

Antarctic Diogenites

Two important observations emerge from our analyses of Antarctic diogenites (Table 4). The first concerns the diversity of their chemical compositions, and the second the presence of possible groupings within these meteorites samples. For the sake of clarity we will first discuss the chemical features of these different groups and then those seen in individual samples.

Asuka-81526–EETA79002 Group

EETA79002 is a complex breccia that contains materials from at least three different diogenitic lithologies, including an olivine-rich orthopyroxenite (Mittlefehldt 2000). Mittlefehldt (2000) has analyzed the trace element abundances of 16 chips of this meteorite, and found a remarkably uniform incompatible lithophile element distribution. We have analyzed one more chip of EETA79002, and our analysis is similar to these earlier results. Furthermore, the REE patterns of the various chips (Mittlefehldt 2000 and this study) and the average composition of orthopyroxene obtained in-situ by SIMS (Fowler et al. 1995) are strikingly similar (Fig. 6a).

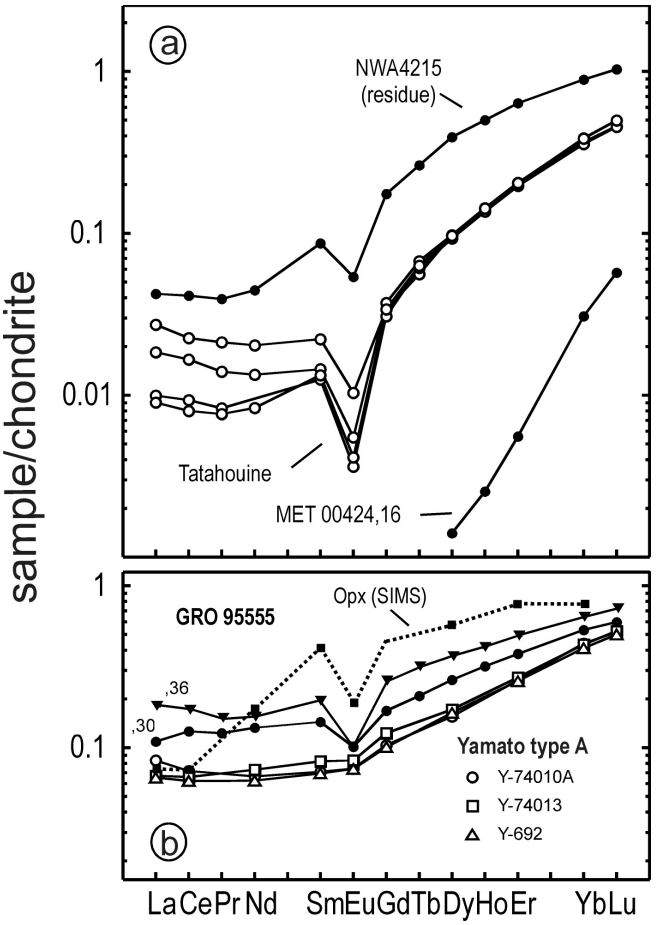

Fig. 4. REE patterns of the Tatahouine (Barrat et al. 1999 and this study), MET 00424, GRO 95555 diogenites. The patterns of the Yamato-A (Masuda et al. 1979), NWA 4215 (Barrat et al. 2006) diogenites and the average orthopyroxene from GRO 95555 (Papike et al. 2000) are shown for comparison. The reference chondrite is from Evensen et al. (1978). The 2σ errors for the new analyses are equivalent to the size of the data points.

An important outcome of our analysis is the discovery that six of the Antarctic diogenites display incompatible lithophile element distributions very similar to that seen in EETA79002. These samples are: A-881526, LaPaz Icefield (LAP) 02216, LAP 03569, LAP 03630, MET 00422, and Miller Range (MIL) 03368. Among them, LAP 03569 and MET 00422 exhibit slightly less pronounced light REE depletions, however, these differences are not important (Figs. 6b and 6c). We did not expected such a grouping, in part because of the diversity of the REE patterns previously obtained for the diogenites and their pyroxenes (e.g., Mittlefehldt 1994; Fowler et al. 1995), and because of the possible involvement of a light REE-rich component able to alter the shape of the REE patterns (see above). Among these stones, only LAP 02216 and LAP 03569 were previously known to be paired. However, textural and phase composition differences among the other stones suggests that they are distinct meteorites and cannot be paired; see *Antarctic*

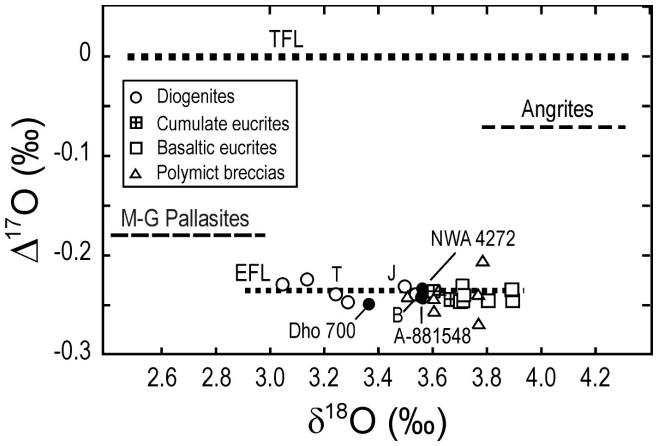

Fig. 5. Oxygen isotope variation in diogenites and eucrites. All $\Delta^{17}O$ values are linearized (see text for details). The data set is limited to analyses obtained in Open University to avoid analytical bias (Greenwood et al. 2005, 2006; Barrat et al. 2006, 2007 and this study). For clarity, error bars for individual analysis have been omitted. (EFL = eucrite fractionation line, TFL = terrestrial fractionation line, B = Bilanga, J = Johnstown, T = Tatahouine).

Meteorite Newsletter (JSC, Houston) 26, 2 (2003), 27, 3 (2004), 28, 1 (2005) and *Meteorite Newsletter* (NIPR, Tokyo) 13, 1 (2005).

The uniformity of the trace incompatible lithophile element distributions of EETA79002 (Mittlefehldt 2000) and of the other diogenites in this group indicates that the contribution of a trapped melt (or another light REE enriched phase) is at best very limited. It can be inferred that they either originated from the same magmatic system, or from very similar parental melts.

Asuka-881839–MET 00425–MET 00436 Group

These three diogenites are compositionally very different: MET 00425 is the most Mg-rich diogenite analyzed so far; MET 000436 and A-881839 are among the most Fe-rich ones. Their lithophile trace element abundances are extremely different and do not follow the major element compositions, as portrayed by the REE concentrations. MET 00425 and A-881839 have respectively about 2 times and 20 times more REEs than MET 00436. Despite these differences, they have been grouped together because they share a remarkable characteristic (Fig. 7a): their REE patterns are fairly flat and display similar negative Eu anomalies (La_n/Sm_n = 0.75–0.84, Eu/Eu^* = 0.43–0.50). Such features are unusual and strongly suggest the involvement of light-REE rich component(s). Indeed, MET 00425 and MET 00436 both exhibit a slight positive Ce anomaly. This kind of anomaly has been documented previously in weathered Antarctic finds (Shimizu et al. 1984; Floss and Crozaz 1991; Mittlefehldt and Lindstrom 1991, 2003) and has been ascribed to the dissolution of REE-rich phosphates by water equilibrated with the atmosphere (Mittlefehldt and Lindstrom 1991). Ce can be oxidized to the +4 state, and in this way becomes

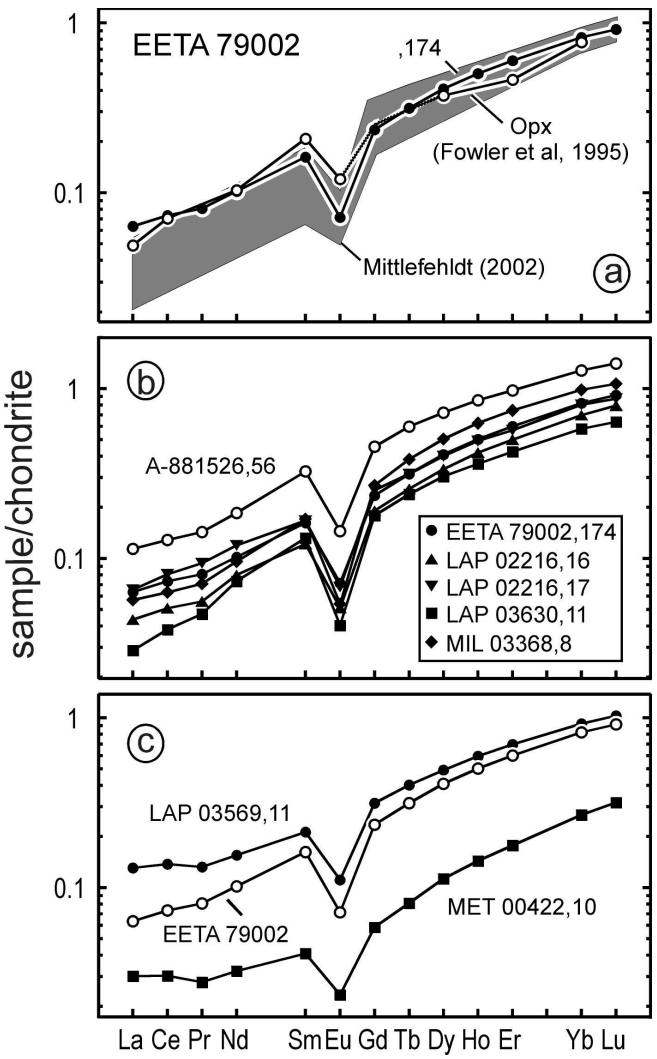

Fig. 6. REE patterns of the EETA79002 group diogenites (EETA79002, LAP 02216, LAP 03569, LAP 03630, MET 00422, MIL 03368, A-881526). The field of the results for EETA79002 obtained by Mittlefehldt (2000) on 16 different chips, and by Fowler et al. (1995) on orthopyroxene by ion-probe are shown for comparison. The reference chondrite is from Evensen et al. (1978). The 2σ errors for the new analyses are equivalent to the size of the data points.

fractionated from the +3 charged REEs. Thus, weathering of Antarctic meteorites generates a variety of REE patterns, some exhibiting positive, and some negative Ce anomalies. Here, the positive Ce anomalies can be interpreted as the possible fingerprint of REE-rich phosphates in these two MET diogenites. Although scarce, these phases have been observed in Roda, Bilanga and Manegaon (Mittlefehldt 1994; Domanik et al. 2004, 2005).

To verify whether a REE-rich phase was present in these diogenites, we have leached the remaining powder (83 mg) obtained from our allocated chip of A-881839 using hot 7N HNO_3 (120 °C) for 20 min. The residue (rinsed 5 times in ultrapure water) and the HNO_3 fraction were both analyzed for trace elements and P. The HNO_3 fraction contained detectable amounts of P (about 1 μg of P), which confirmed that a phosphate phase has been leached. Consequently, we adjusted the abundances of the other elements in this fraction assuming a P_2O_5 concentration fixed to 42 wt%. This fraction is named "phosphate" (Table 4), and is either enriched or highly enriched in Sr, Y, Zr, Nb, Ba, REEs, Hf, Th, and U. Its REE pattern (Fig. 7b) is light-REE enriched ($La_n/Yb_n = 7.05$) and displays a distinct positive Eu anomaly ($Eu/Eu^* = 1.19$). The latter is probably not related to the phosphate phase, but is more likely produced by a small amount of plagioclase dissolved in the hot HNO_3. Nevertheless, the REE concentrations displayed by the "phosphate" fraction are very high and in the range expected for whitlockite. The residue displays lower concentrations in Sr, Y, Ba, light REEs, and Th, and also lower Co, Ni, and Cu concentrations than the unleached sample, suggesting that a small amount of metal and sulfide had been dissolved (Table 3). The REE pattern of the residue (Fig. 7b) is in agreement with an orthopyroxene composition, with a significant light REE depletion ($La_n/Sm_n = 0.26$) and a deep negative Eu anomaly ($Eu/Eu^* = 0.12$). The trace element content of the bulk sample is well accounted for by a mixture of 99.993 wt% residue and only 0.007 wt% "phosphate."

Asuka-881548

A-881548 is a diogenite that contains inhomogeneously distributed olivine grains (up to 70 vol% in a 1 cm^2 section). The major element abundances measured in this study indicate that our allocated chip was devoid of olivine. The distribution of the lithophile incompatible trace elements of A-881548 are unlike the previous samples. However, its REE pattern resembles the residue of A-881839 (Fig. 7c) with a similar light REE depletion ($La_n/Sm_n = 0.30$) but a less pronounced negative Eu anomaly ($Eu/Eu^* = 0.37$). The bulk oxygen isotopic composition of A-881548 has been determined on both untreated and ethanolamine thioglycollate-washed samples (Table 5). The very good agreement between these samples indicates that A-881548 has experienced very low degrees of terrestrial weathering. The oxygen isotope analysis for the acid washed sample (Fig. 5) is well within the range of previous measurements from diogenites (Clayton and Mayeda 1996; Wiechert et al. 2004; Greenwood et al. 2005).

Grosvenor Mountains 95555

This unbrecciated diogenite was previously studied by Papike et al. (2000). The REE patterns of our two chips and the average composition of orthopyroxene obtained in-situ by SIMS by these authors are not similar (Fig. 4b), and we have no satisfactory explanation for this discrepancy. Interestingly, the shapes of the REE patterns we have obtained are akin to that obtained for the Yamato-type A diogenites (Masuda et al. 1979). GRO 95555, however, exhibits more pronounced

negative Eu anomalies. One of the analyzed chips (GRO 95555,30), displays a slight positive Ce anomaly ($Ce/Ce^* = 1.08$, Antarctic weathering involving minute amounts of phosphate?). Indeed, minute amounts of phosphates could explain the different REE abundances displayed by the chips ,30 and ,36.

MET 00424

This ferroan diogenite (FeO/MgO = 0.80) was by far the most difficult to analyze for trace elements. MET 00424 is the diogenite that displays the lowest incompatible lithophile element concentrations (Mittlefehldt 2002). The concentrations of Zr, Hf, light REEs, Th, U were so low, that we were unable to quantify them correctly. The concentrations we have obtained for heavy REEs and Y are extremely low: only 5 ng/g for Yb, only 6 ng/g for Y. For comparison, Shalka, the diogenite with the lowest heavy REE contents measured before has about 30 ng/g Yb. 19 ng/g Y were measured in an orthopyroxene grain from Ellemeet (Mittlefehldt 1994; Fowler et al. 1995). MET 00424 is not only the sample with the lowest incompatible trace element abundances, it displays the most fractionated heavy REE pattern ($Dy_n/Yb_n = 0.046$, Fig. 4a).

How Many Parental Melts for Diogenites?

While the cumulate origin of diogenites is widely accepted, the number and the composition of their parental melts are still a matter of debate. Two distinct views have been put forward to explain the origin of diogenites and their relationship to eucrites. Many workers (Mason 1967; Bartels and Grove 1991; Warren 1997; Righter and Drake 1997; Ruzicka et al. 1997) have suggested that eucrites and diogenites were directly cogenetic, sharing the same parental melts. In this model diogenites are cumulates that formed during the crystallization of relatively primitive magmas, while eucrites are viewed as the products of more evolved residual melts. In contrast, it has been proposed that diogenites and eucrites are not directly related (e.g., Stolper 1977; Mittlefehldt 1994, 2000; Fowler et al. 1995; Shearer et al. 1997; Barrat 2004), with diogenites representing cumulates from parental melts for which the composition cannot be easily constrained (ultramafic melts? Mg-rich basalts or Mg-rich andesites?).

Incompatible element systematics, while extremely useful for bulk rocks that represent melt compositions, are more ambiguous for cumulate rocks. However, our new results extend the range of known diogenite compositions, and can constrain some features of their parental melts:

1. Trace and major element abundances are rarely coupled in diogenites. A correlation between Sc and FeO/MgO ratios has been previously noticed (Göpel and Wänke 1978; Mittlefehldt 2002) and is confirmed by the present data (Fig. 8a). However, Sc is well correlated with the Fe or Mn abundances and so a relationship of the type displayed by Fig. 8 does not necessarily have any petrogenetic significance. If diogenites are part of a single crystallization sequence then clear relationships between incompatible trace elements (e.g., the REEs) and differentiation indexes (e.g., the FeO/MgO ratios) are to be expected, but none has been observed (Fig. 8b). The involvement of an incompatible rich component (e.g., a trapped melt), or metamorphic equilibration are both plausible explanations for the absence of such correlations (Mittlefehldt 1994). However, it is also possible that the spread of the data in the Yb versus FeO/

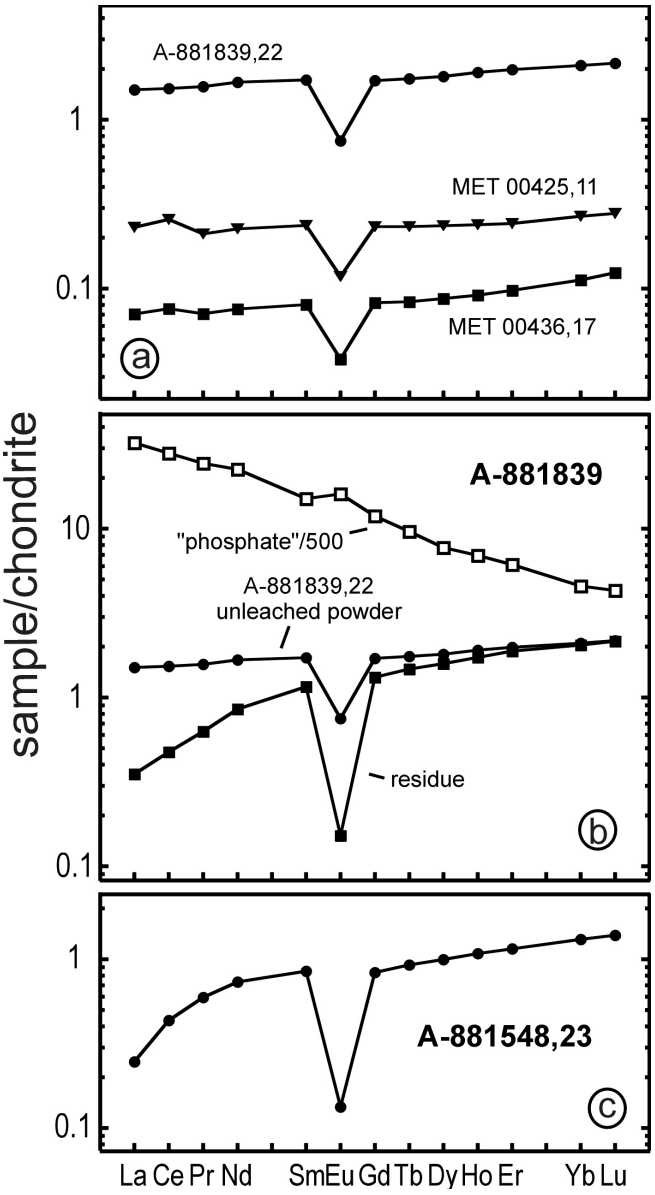

Fig. 7. REE patterns of the diogenites Asuka-881548, A-881839, MET 00425, and MET 00436. A-881839 has been leached and the residue and the leachate ("phosphate") were analyzed (see the text for more details). The reference chondrite is from Evensen et al. (1978). The 2σ errors are equivalent to the size of the data points.

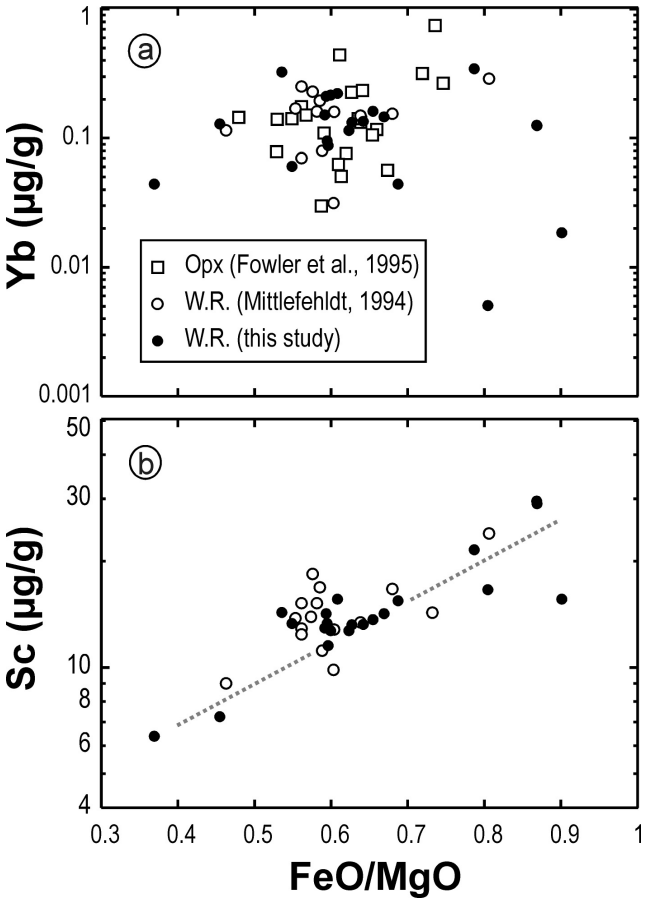

Fig. 8. Yb and Sc versus FeO/MgO (wy%/wt%) diagrams for diogenites (W.R.: whole rock, Opx: average orthopyroxene). The 2σ errors for the new analyses are equivalent to the size of the data points.

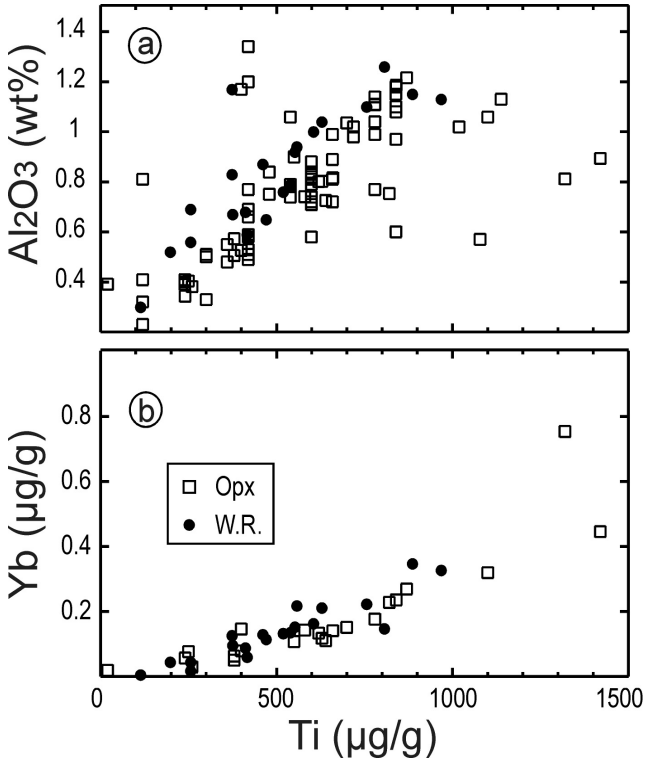

Fig. 9. Al_2O_3 and Yb versus Ti diagrams for diogenites (W.R.: whole rock, Opx: average orthopyroxene). The data are mainly from Berkley and Boynton (1992), Mittlefehldt (1994, 2000), Fowler et al. (1994, 1995), Domanik et al. (2003), Liermann and Ganguly (2001), Barrat et al. (1999, 2006) and this study. The 2σ errors for the new analyses are equivalent to the size of the data points.

MgO plot (Fig. 8b) reflects the pristine distribution, and hence is indicative of a real diversity within the parent melts that produced the diogenites.

2. Previous studies have shown that Al, Zr, Y, Yb, and Ti abundances in diogenites exhibit significant linear relationships (Fig. 9). These variations are at first glance consistent with igneous fractionation from a common parent melt. However, this interpretation is unlikely as it implies high degrees of fractional crystallization, using either constant or increasing partition coefficients with decreasing temperature. Such high degrees of fractional crystallization are inconsistent with the nearly monomineralic composition of most diogenites and the scarcity of plagioclase which is expected to crystallize abundantly if a Mg-rich basaltic parent melt is assumed (Mittlefehldt 1994; Fowler et al. 1995). Alternatively, the linear trends could be also generated by fractional crystallization of different melts (e.g., Fowler et al. 1995). In addition, it can be seen from Fig. 9 that many pyroxene analyses plot significantly away from the main trend in the Al versus Ti diagram, a feature which supports the idea that multiple parental melts were involved in the genesis of the diogenites.
3. The low-Ca pyroxene KD (about 0.27) is well determined for eucritic or high-Mg eucritic systems (Stolper 1979; Bartels and Grove 1991). In principle, using this value, the Fe/Mg ratio of the melt in equilibrium with crystals can be deduced only if their distribution of Fe or Mg has not been affected by reaction with interstitial melt, subsolidus or metamorphic re-equilibrations, or any post-crystallization process. Most orthopyroxene crystals in diogenites are homogeneous with respect to major elements. It could therefore be suggested that any initial zoning was erased by later metamorphic processes (e.g., Mittlefehldt 1994). If this interpretation was correct, any estimate of the Fe/Mg ratio of their parent melt would be seriously in error. However, in the case of cumulates, there are many factors that determine the extent of the zoning in the cumulus phases. Of particular importance is the fraction of trapped melt. If this fraction is significant, crystals can develop large rims with evolved compositions. If the melt has been almost totally expelled, as is the case for the diogenites (e.g., Barrat 2004), zoning can be far less pronounced, or the volume of rim material highly restricted compared to that of the core. In other words, the average composition of the crystals may not necessarily be far removed from that of their core and

hence can provide useful constraints on the composition of the parent melt. Pyroxenes that still display pristine zoning with respect to Fe and Mg, have been found in two diogenites, Garland and NWA 4215. In the first case, the average core and rim compositions are not very different (respectively $En_{72.4}$ and $En_{69.4}$, Fowler et al. 1994). For NWA 4215 (Barrat et al. 2006), the composition of a typical crystal ranges from $En_{76.2}$ to $En_{71.4}$, and the average composition is close to $En_{74.0}$. These two examples suggest that the average compositions of orthopyroxene crystals in diogenites are strongly controlled by the composition of their cores. Hence, the FeO/MgO ratios of their parent melts can be estimated from the composition of average pyroxenes or whole rocks. Using literature data (Mittlefehldt 1994; Fowler et al. 1994), and the whole rock compositions obtained in this study, we calculate that the FeO/MgO ratios of diogenite parental melts ranged from about 1.4 to 3.5 (Fig. 10). In our calculations we have assumed that diogenites contain only orthopyroxene, however, taking into account the involvement of chromite or olivine would not significantly alter these values. This range of values is wide and overlaps that obtained for non-cumulate eucrites. It is possible to question the validity of these calculations and suggest that the Fe/Mg ratio of the initial core of the crystals and that of the average pyroxene could be very different, especially for some of the most ferroan diogenites (like the unique Dhofar 700 whose pyroxenes exhibit preserved zonings for Al, Cr, Ca and possibly Ti). Nevertheless, the wide range of FeO/MgO ratios calculated for equilibrium melts is certainly not an artifact, and reflects the diversity of the parental melts involved. We note that the FeO/MgO ratios of many calculated melts cluster around 2–2.5, a value very similar to some main-group eucrites. This could indicate that many diogenites formed from melts with FeO/MgO ratios close to those that produced the eucrites, but of course with a different composition. In other words, the parent melts of diogenites were not systematically more "primitive" than the eucrites. We note that the range of the FeO/MgO ratios of the cores of the pigeonite crystals from the unequilibrated eucrites (FeO/MgO = 0.63–1.39, Pun and Papike 1996) overlaps partly the values obtained for diogenites (FeO/MgO = 0.36–0.90), which is in full agreement with this interpretation. This conclusion is at odds with a simple magma ocean model, in which the diogenites are seen as being the early-formed cumulates from a relatively primitive magma which as a consequence underwent progressive differentiation to produce the more evolved liquids that gave rise to the eucrites.

4. We have tentatively calculated the abundances of Yb and the $(Dy/Yb)_n$ ratios of the parental melts of diogenites using the partition coefficients for orthopyroxene obtained experimentally by Schwandt and McKay (1998). The spread of the results displayed in the Yb versus FeO/MgO plot (Fig. 10) cannot be solely explained by secondary processes (metamorphic reequilibration, trapped melt effects, etc.), and indicates again a diversity of parental melts for diogenites. This is further confirmed by the range of their calculated $(Dy/Yb)_n$ ratios (Fig. 10), in particular because Barrat (2004) has shown that these ratios are not very sensitive to the influence of trapped melt. Indeed, the results obtained here indicate unambiguously that some diogenites (e.g., Tatahouine and MET 00424) formed from melts characterized by a significant heavy REE enrichment (i.e., $(Dy/Yb)_n < 1$). Such a feature clearly demonstrates that basaltic eucrites and these diogenites could not have originated from the same parental melts. Furthermore,

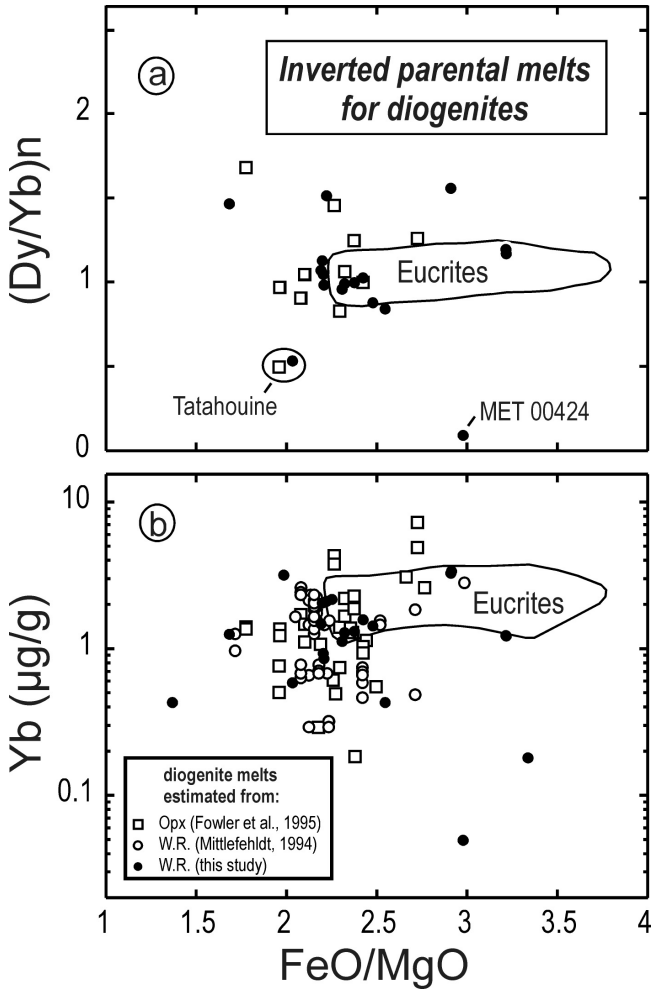

Fig. 10. $(Dy/Yb)_n$ and Yb versus FeO/MgO diagrams for the calculated parental melts of diogenites (see the text for more details). The samples (WR) that contain a light REE rich component are not shown in the $(Dy/Yb)_n$ versus FeO/MgO plot. The field for basaltic eucrites is drawn from literature data (mainly from Barrat et al. 2003, 2007).

some parental melts are characterized by $(Dy/Yb)_n > 1$. Such results are not necessarily reliable when obtained from bulk rock concentrations. If the rock contains a light REE rich component, the Dy/Yb ratios of the bulk rock and of the orthopyroxene are different. This is exemplified by Johnstown (Fig. 2) and the leaching experiment performed on A-881839 (Fig. 7b). For this reason, samples where a light REE-rich component was suspected, are not used in the $(Dy/Yb)_n$ versus FeO/MgO plot (Fig. 10). For melts calculated from the orthopyroxene compositions obtained by ion-probe (Fowler et al. 1995), this inference has greater validity. Alternatively, these high $(Dy/Yb)_n$ ratios could be partly explained by the involvement of a significant fraction of trapped melts (about 10–20 wt% of trapped melts are required (Barrat 2004)). However, textural and chemical evidence indicates that, if present, the amount of trapped melt in diogenites was minor, and probably not sufficient to alter drastically the Dy/Yb ratios of the orthopyroxenes (Barrat 2004).

Our new results are consistent with the conclusions of previous studies suggesting that there is no direct genetic link between diogenites and eucrites (e.g., Stolper 1977; Mittlefehldt 1994, 2000; Fowler et al. 1995; Shearer et al. 1997; Barrat 2004). The behavior of heavy REEs demonstrates unambiguously that a variety of parental melts are required to account for the composition of diogenites. The diversity of the trace element abundances displayed by diogenites cannot be explained by a simple single-stage magma ocean model, nor by the involvement of a single large magma reservoir. Of major importance, we confirm that some diogenites such as Tatahouine or MET 00424, formed from melts displaying a pronounced heavy REE enrichment, a feature which is necessarily inherited from their sources. Two hypotheses can be proposed for the origin of such heavy REE enrichments (the reader is referred to Barrat (2004) for a more detailed discussion of this topic). First, a residue from which significant melt has been extracted, which prior to melting had a flat REE pattern, will then have a $Dy/Yb)_n$ ratio significantly lower than 1. Remelting of such a residue could in theory produce a HREE-enriched liquid. This is essentially the model for the genesis of the diogenites proposed by Stolper (1977). Alternatively, olivine and pyroxene rich cumulates formed from melts displaying a flat REE pattern would also exhibit strong heavy REE enrichment. Remelting of such a cumulate pile would also generate melts displaying a variety of $(Dy/Yb)_n$ ratios, including very low values.

Oxygen isotope evidence presented here and previously (Greenwood et al. 2005) demonstrates that all lithologies of the HED suite, including the diogenites, have an extremely restricted $\Delta^{17}O$ composition consistent with a large scale homogenization event early in the history of Vesta. The most likely scenario to explain this homogenization event is planetary-scale melting of the type that would have led to the formation of a magma ocean. Under such circumstances, a model that produces the eucrites by relatively low degrees of partial melting followed by remelting of the remaining source region to produce diogenitic parental melts (Stolper 1977) would appear to be untenable. This suggests that the HREE enriched trace element patterns seen in diogenites, such as Tatahouine or MET 00424 (Fig. 4), must necessarily involve remelting of previously formed cumulates. At first sight, this would appear to be at odds with the progressive crystallization of a magma ocean. However, we presently have little information about the crustal structure of Vesta and an extremely poor understanding of the stages in the development of any early-formed global magma ocean (Righter and Drake 1997; Warren 1997). It is possible that the initial crustal layer of the magma ocean would have comprised eucritic volcanic rocks underlain by a relatively thick pile of hot cumulates. Underneath this initial carapace the still primitive and therefore hot magma ocean would have been undergoing relatively rapid convection and hence be relatively well-mixed both compositionally and thermally. Foundering and entrainment of portions of the hot cumulate pile into the underlying magma ocean would be highly likely and where a significant density contrast exists such fragments would sink to the base of the global magma chamber. However, the base of the cumulate pile would have been relatively hot and the thermal contrast between it and the underlying ocean relatively small. Under such conditions, the cumulate pile would at least locally have experienced significant degrees of melting. Once formed there would have been two possible routes for any melt produced by this process. It would either have become entrained in the convecting magma ocean, or more likely due to the density contrast with the overlying crust it would have intruded the overlying crust as diapirs. While this is a speculative scenario due to our lack of understanding of the processes on early Vesta, it is entirely feasible that significant amounts of remelting of the early formed crust took place on Vesta.

SUMMARY AND IMPLICATIONS FOR HED METEORITES

Major and trace element abundances were determined for 18 diogenites using ICP-AES and ICP-MS. This new data set extends the range of known diogenite compositions, from Mg-rich examples (e.g., MET 00425) to Mg-poor diogenites (e.g., Dhofar 700 and MET 00436). In agreement with previous analyses on bulk rocks, the diogenites display a wide range of trace element abundances (Fukuoka et al. 1977; Wolf et al. 1983; Mittlefehldt 1994, 2000). Such variations are partly explained by the inhomogeneous distribution of accessory phases such as sulfides and metal for chalcophile or siderophile elements, and phosphates in some cases for incompatible elements. Apart from a few samples that display the fingerprint of light REE-rich phases (e.g., Johnstown NWA 4272, MET 00425, MET 00436, and A-881839), the range of incompatible element abundances, and particularly

the range of Dy/Yb ratios in diogenites is best explained by the diversity of their parental melts. Indeed, the data presented here confirm that some diogenites formed from heavy REE-enriched melts. The diversity of the parental melts required to explain the chemical features of diogenites indicates that they have not crystallized in a single magmatic system.

To date, no possible parental melt for diogenites has been identified among the 800 known HED meteorites. Compared to the proportions of diogenites and howardites that contain numerous clasts of diogenites (more than 40% of the HED population), this lack of a potential parental composition is disturbing. Why have such materials not yet been found? At least three potential reasons can be suggested (Mittlefehldt and Lindstrom 1998): (1) It could be suggested that these melts have never been emitted as lavas on the surface of the parent body, but rather crystallized at depth, below or into the eucritic crust. If this were the case, we should have a significant number of samples from these intrusive complexes that crystallized from the residual liquids formed after the extraction of diogenites, and such samples are also unknown. Furthermore, a fine-grained diogenite that possibly cooled faster than the other diogenites and formed within a small, shallow intrusion has recently been identified (Barrat et al. 2006). Thus, this explanation seems unlikely. (2) It could be proposed that these samples exist but have not yet been identified because their particular features have been erased by an extensive metamorphism and/or brecciation; (3) alternatively, lavas genetically linked to diogenites are exposed somewhere on Vesta, but are totally lacking in the HED collection.

It is often assumed that the HED meteorites provide a reliable picture of the lithologic diversity exposed at the surface of Vesta. If rocks with the composition of the parental melts of diogenites are not present in the HED collection, then this assumption is probably invalid. Indeed, cosmic-ray exposure ages for the HEDs suggest that all these meteorites are associated with only five impact events (Welten et al. 1997), a number that is probably insufficient to sample all the geological diversity of the entire surface of the body. The recent discovery of K-rich impact glasses in howardites demonstrates that the rocks that crop out on Vesta are certainly not restricted to eucrites and ultramafic cumulates (Barrat et al., Forthcoming). The remote sensing studies that will be performed during the Dawn mission, should help to confirm the petrological diversity of the exposed lithologies, and identify the chemically different areas present on Vesta.

Acknowledgments—We thank R. Korotev for the editorial handling, H. McSween, M. J. Krawczynski for constructive comments, and Pascale Barrat for her help. We gratefully acknowledge the Programme National de Planétologie (INSU) and the Science and Technology Facilities Council (STFC) for financial support, and the NASA meteorite working group, the NIPR, the AMNH (J. Boesenberg), Alain Carion, and Michel Franco, for providing the samples. This research has made use of NASA's Astrophysics Data System Abstract Service. Jenny Gibson is thanked for her assistance with oxygen isotope analysis.

Editorial Handling—Dr. Randy Korotev

REFERENCES

Barrat J. A. 2004. Determination of the parental magmas of HED cumulates: The effects of interstitial melts. *Meteoritics & Planetary Science* 39:1767–1779.

Barrat J. A., Gillet Ph., Lesourd M., Blichert-Toft J., and Poupeau G. R. 1999. The Tatahouine diogenite: Mineralogical and chemical effects of sixty-three years of terrestrial residence. *Meteoritics & Planetary Science* 34:91–97.

Barrat J. A., Blichert-Toft J., Gillet Ph., and Keller F. 2000a. The differentiation of eucrites: The role of in-situ crystallization. *Meteoritics & Planetary Science* 35:1087–1100.

Barrat J. A., Boulègue J., Tiercelin J. J., and Lesourd M. 2000b. Strontium isotopes and rare-earth element geochemistry of hydrothermal carbonate deposits from Lake Tanganyika, East Africa. *Geochimica et Cosmochimica Acta* 64:287–298.

Barrat J. A., Jambon A., Bohn M., Blichert-Toft J., Sautter V., Göpel C., Gillet Ph., Boudouma O., and Keller F. 2003. Petrology and geochemistry of the unbrecciated achondrite Northwest Africa 1240 (NWA 1240): An HED parent body impact melt. *Geochimica et Cosmochimica Acta* 67:3959–3970.

Barrat J. A., Beck P., Bohn M., Cotten J., Gillet Ph, Greenwood R. C., and Franchi I. A. 2006. Petrology and geochemistry of the fine-grained, unbrecciated diogenite Northwest Africa 4215. *Meteoritics & Planetary Science* 41:1045–1057.

Barrat J. A., Yamaguchi A., Greenwood A., Bohn M., Cotten J., Benoit M., and Franchi I. A. 2007. The Stannern trend eucrites: Contamination of main group eucritic magmas by crustal partial melts. *Geochimica et Cosmochimica Acta* 71:4108–4124.

Barrat J. A., Bohn M., Gillet Ph., and Yamaguchi A. Forthcoming. Evidence for K-rich terrains and granites on Vesta from impact spherules. *Meteoritics & Planetary Science* 44.

Bartels K. S. and Grove T. L. 1991. High pressure experiments on magnesian eucrite compositions: Constraints on magmatic processes in the eucrite parent body. Proceedings, 21st Lunar and Planetary Science Conference. pp. 351–365.

Berkley J. L. and Boynton N. J. 1992. Minor/major element variation within and among diogenite and howardite orthopyroxenite groups. *Meteoritics* 27:387–394.

Binzel R. P., Gaffey M. J., Thomas P. C., Zellner B. H., Storrs A. D., and Wells E. N. 1997. Geologic mapping of Vesta from 1994 Hubble Space Telescope images. *Icarus* 128:95–103.

Bunch T. E., Wittke J. H., D. Rumble III, Irving A. J., and Reed B. 2006. Northwest Africa 2968: A dunite from Vesta (abstract #5252). 69th Annual Meeting of the Meteoritical Society. *Meteoritics & Planetary Science* 41:A31.

Connolly H. C., Smith C., Benedix G., Folco L., Righter K., Zipfel J., Yamaguchi A., and Chennaoui Aoudjehane H. 2007. The Meteoritical Bulletin, No. 92, 2007, September. *Meteoritics & Planetary Science* 42:1647–1694.

Consolmagno G. J. and Drake M. J. 1977. Composition and evolution of the eucrite parent body: Evidence from rare earth elements. *Geochimica et Cosmochimica Acta* 41:1271–1282.

Cornish L. and Doyle A. 1984. Use of ethanolamine thioglycollate in the conservation of pyritized fossils. *Palaeontology* 27:421–424.

Cotten J., Ledez A., Bau M., Caroff M., Maury R. C., Dulski P.,

Fourcade S., Bohn M., and Brousse R. 1995. Origin of anomalous rare-earth element and yttrium enrichments in subaerially exposed basalts—Evidence from French Polynesia. *Chemical Geology* 119:115–138.

Desnoyers C. 1982. L'olivine dans les howardites: Origine, et implications pour le corps parent de ces meteorites achondritiques. *Geochimica et Cosmochimica Acta* 46:667–680.

Domanik K., Kolar S., Musselwhite D., and Drake M. J. 2004. Accessory silicate mineral assemblages in the Bilanga diogenite: A petrographic study. *Meteoritics & Planetary Science* 39:567–579.

Domanik K., Sideras L. C., and Drake M. J. 2005. Olivine and Ca-phosphates in the diogenites Manegaon and Roda (abstract #2128). 36th Lunar and Planetary Science Conference. CD-ROM.

Evensen N. M., Hamilton P. J., and O'Nions R. K. 1978. Rare earth abundances in chondritic meteorites. *Geochimica et Cosmochimica Acta* 42:1199–1212.

Fredriksson K., Noonan A., Brenner P., and Sudre C. 1976. Bulk and major phase composition of eight hypersthene achondrites. *Meteoritics* 11:278–280.

Floran R. J., Prinz M., Hlava P. F., Keil K., Spettel B., and Wänke H. 1981. Mineralogy, petrology, and trace element geochemistry of the Johnstown meteorite: A brecciated orthopyroxenite with siderophile and REE-rich components. *Geochimica et Cosmochimica Acta* 45:2385–2391.

Fowler G. W., Papike J. J., Shearer C. K., and Spilde M. N. 1994. Diogenites as asteroidal cumulates. Insights from orthopyroxene major and minor element chemistry. *Geochimica et Cosmochimica Acta* 58:3921–3929.

Fowler G. W., Papike J. J., Spilde M. N., and Shearer C. K. 1995. Diogenites as asteroidal cumulates. Insights from orthopyroxene trace element chemistry. *Geochimica et Cosmochimica Acta* 59: 3071–3084.

Fukuoka T., Boynton W. V., Ma M. S., and Schmitt R. A. 1977. Genesis of howardites, diogenites and eucrites. Proceedings, 8th Lunar Science Conference. pp. 187–210.

Gaffey M. J. 1997. Surface lithologic heterogeneity of asteroid 4-Vesta. *Icarus* 127:130–157.

Göpel C. and Wänke H. 1978. Trace elements in single pyroxene crystals of diogenites, howardites and eucrites. *Meteoritics* 13: 477–480.

Greenwood R. C., Franchi I. A., Jambon A., and Buchanan P. C. 2005. Widespread magma oceans on asteroidal bodies in the early solar system. *Nature* 435:916–918.

Greenwood R. C., Franchi I. A., Jambon A., Barrat J. A., and Burbine T. H. 2006. Oxygen isotope variations in stony-iron meteorites. *Science* 313:1763–1765.

Hewins R. H. 1988. Equilibration of foreign clasts in the Peckelsheim diogenite (abstract). 19th Lunar and Planetary Science Conference. pp. 485–486.

Ikeda Y. and Takeda H. 1985. A model for the origin of basaltic achondrites based on the Yamato-7308 howardite. Proceedings, 15th Lunar and Planetary Science Conference. *Journal of Geophysical Research* 90:C649–C663.

Ionov D. A., Prikhodko V. S., Bodinier J. L., Sobolev A. V., and Weis D. 2005. Lithospheric mantle beneath the Southeast Siberian craton: Petrology of peridotites xenoliths in basalts from Tokinsky Stanovik. *Contributions to Mineralogy and Petrology* 149:647–665.

Jérome D. Y. and Christophe Michel-Lévy M. 1972. The Washougal meteorite. *Meteoritics* 7:449–461.

Lacroix A. 1932. La meteorite (diogénite) de Tataouine, Tunisie (27 juin 1931). *Bulletin de la société française de Minéralogie et Cristallographie* 55:101–122.

Liermann H. P. and Ganguly J. 2001. Compositional properties of coexisting orthopyroxene and spinel in some Antarctic diogenites: Implications for thermal history. *Meteoritics & Planetary Science* 36:155–166.

Lomena I. S. M., Touré F., Gibson E. K. Jr., Clanton U. S., and Reid A. M. 1976. Aïoun el Atrouss: A new hypersthene achondrite with eucritic inclusions. *Meteoritics* 11:51–57.

Makishima A. and Nakamura E. 1997. Suppression of matrix effects in ICP-MS: Application to precise determination of Rb, Sr, Y, Cs, Ba, REE, Pb, Th and U at ng.g-1 levels in milligram silicate samples. *Geostandards Newsletter* 21:307–319.

Mason B. 1967. The Bununu achondrite, and a discussion of the pyroxene-plagioclase achondrites. *Geochimica et Cosmochimica Acta* 31:107–115.

Masuda A., Tanaka T., Shimizu H., Wakisaka T., and Nakamura N. 1979. Rare-earth geochemistry of Antarctic diogenites. *Memoirs of the National Institute of Polar Research* 15:177–188.

McCord T. B., Adams J. B., and Johnson T. V. 1970. Asteroid Vesta: Spectral reflectivity and compositional implications. *Science* 168:1445–1447.

Miller, M. F. 2002. Isotopic fractionation and the quantification of ^{17}O anomalies in the oxygen three-isotope system: An appraisal and geochemical significance. *Geochimica et Cosmochimica Acta* 66:1881–1889.

Miller M. F., Franchi I. A., Sexton A. S., and Pillinger C. T. 1999. High precision $\Delta^{17}O$ delta 0–17 isotope measurements of oxygen from silicates and other oxides: Method and applications. *Rapid Communications in Mass Spectrometry* 13:1211–1217.

Mittlefehldt D. W. 1979. Petrographic and chemical characterization of igneous lithic clasts from mesosiderites and howardites and comparison with eucrites and diogenites. *Geochimica et Cosmochimica Acta* 43:1917–1935.

Mittlefehldt D. W. 1994. The genesis of diogenites and HED parent body petrogenesis. *Geochimica et Cosmochimica Acta* 58:1537–1552.

Mittlefehldt D. W. 2000. Petrology and geochemistry of the Elephant Moraine A79002 diogenite: A genomict breccia containing a magnesian harzburgite component. *Meteoritics & Planetary Science* 35:901–912.

Mittlefehldt D. W. 2002. Geochemistry of new, unusual diogenites and constraints on diogenite genesis (abstract). 65th Annual Meeting of the Meteoritical Society. *Meteoritics & Planetary Science* 37:A100.

Mittlefehldt D. W. and Lindstrom M. M. 1998. Black clasts from howardite QUE 94200—Impact melts, not primary magnesian basalts (abstract #1832). 29th Lunar and Planetary Science Conference. CD-ROM.

Mittlefehldt D. W. and Lindstrom M. M. 2003. Geochemistry of eucrites: Genesis of basaltic eucrites, and Hf and Ta as petrogenetic indicators for altered Antarctic eucrites. *Geochimica et Cosmochimica Acta* 67:1911–1935.

Papike J. J., Shearer C. K., Spilde M. N., and Karner J. M. 2000. Metamorphic diogenite Grosvenor Mountains 95555: Mineral chemistry of orthopyroxene and spinel and comparisons to the diogenite suite. *Meteoritics & Planetary Science* 35:875–879.

Pun A. and Papike J. J. 1996. Unequilibrated eucrites and the equilibrated Juvinas eucrite: Pyroxene REE systematics and major, minor, and trace element zoning. *American Mineralogist* 81:1438–1451.

Righter K. and Drake M. J. 1997. A magma ocean on Vesta: Core formation and petrogenesis of eucrites and diogenites. *Meteoritics & Planetary Science* 32:929–944.

Ruzicka A., Snyder G. A., and Taylor L. A. 1997. Vesta as the howardite, eucrite and diogenite parent body: Implications for

the size of a core and for large-scale differentiation. *Meteoritics & Planetary Science* 32:825–840.

Saiki K., Takeda H., and Ishii T. 2001. Mineralogy of Yamato-791192, HED breccia and relationship between cumulate eucrites and ordinary eucrites. *Antarctic Meteorite Research* 14:28–46.

Schwandt C. S. and McKay G. 1998. Rare earth element partition coefficients from enstatite/melt synthesis experiments. *Geochimica et Cosmochimica Acta* 62:2845–2848.

Shearer C. K., Fowler G. W., and Papike J. J. 1997. Petrogenetic models for magmatism on the eucrite parent body: Evidence from orthopyroxene in diogenites. *Meteoritics & Planetary Science* 32:877–889.

Shimizu H., Tanaka T., and Masuda A. 1984. Meteoritic $^{138}Ce/^{142}Ce$ ratio and its evolution. *Nature* 307:251–252.

Stolper E. 1977. Experimental petrology of eucrite meteorites. *Geochimica et Cosmochimica Acta* 41:587–611.

Takeda H. 1997. Mineralogical records of early planetary processes on the howardite, eucrite, diogenite parent body with reference to Vesta. *Meteoritics & Planetary Science* 32:841–853.

Treiman A. H. 1997. The parent magmas of the cumulate eucrites: A mass balance approach. *Meteoritics & Planetary Science* 32:217–230.

Warren P. H. 1997. Magnesium oxide-iron oxide mass balance constraints and a more detailed model for the relationship between eucrites and diogenites. *Meteoritics & Planetary Science* 32:945–963.

Warren P. H. and Jerde E. 1987. Composition and origin of Nuevo Laredo trend eucrites. *Geochimica et Cosmochimica Acta* 51:713–725.

Welten K. C., Lindner L., Van der Borg K., Loeken T., Scherer P., and Schultz L. 1997. Cosmic-ray exposure ages of diogenites and the recent collisional history of the howardite, eucrite and diogenite parent body/bodies. *Meteoritics & Planetary Science* 32:891–902.

Wolf R., Ebihara M., Richter G. R., and Anders E. 1983. Aubrites and diogenites: Trace element clues to their origin. *Geochimica et Cosmochimica Acta* 47:2257–2270.